Journal of Engineering and Development

www.jead.org
Vol. 19, No. 06, November 2015
ISSN 1813-7822

EXPERIMENTAL AND NUMERICAL STUDY OF ENHANCEMENT HEAT TRANSFER COEFFICIENT IN SPIRAL FLUTED TUBE HEAT EXCHANGER WITH NANOFLUID

Muna S. Kassim[1], Fouad A. Salah[2], * Ahmed O.Samarmad[3]

1) Assist Prof., Mechanical Engineering Department, Al-Mustansirya University, Baghdad, Iraq.
2) Assist Prof., Mechanical Engineering Department, Al-Mustansirya University, Baghdad, Iraq.
3) Student, Mechanical Engineering Department, Al-Mustansirya University, Baghdad, Iraq

(Received: 29/3/2015; Accepted: 16/6/2015)

Abstract: Experimental and numerical investigation has been performed in this work to study enhancement of heat transfer coefficient in spiral fluted tube heat exchanger with Nanofluid. The shell side was made from galvanized tube of (65 mm) outer diameter. The tube was made from copper material of (1000 mm) length having (16 mm) equivalent inner diameter and (17 mm) outer diameter, it was inserted inside the shell. Steam was used, as a heating source where constant wall temperature condition (110˚C) was achieved, and TiO_2 /water nanofluid with various volume concentrations (0.08%, 0.1%, 0.2%, and 0.3%) by volume at Reynolds numbers (7000 to 15000) has been employed, as working fluid flows through the inner tube. Fiber glass has been utilized to cover the outer surface of the shell for reducing heat losses. The performance of spiral fluted tube heat exchanger with and without nanofluid was investigated experimentally. Experimental results reveal that the use of spiral fluted tube without nanofluid leads to increase (28-33) % in heat transfer coefficient compared with smooth tube, and the maximum increase in heat transfer coefficient occurs when using spiral fluted tube with nanofluid at 0.3% volume concentration was about (25-28) % higher than the pure water in spiral fluted tube. Empirical correlations for water, nanofluid were represented by Nusselt number. Numerical simulation has been carried out on present heat exchanger to analyze both flow field and heat transfer using ANSYS 14, FLUENT package. The comparison between experimental and numerical results showed good agreement.

Keywords: *heat exchanger, spiral fluted tube, nanofluid*

دراسة عملية و عددية لتحسين أنتقال الحرارة في انبوب لولبي مخدد بوجود المائع النانوي

الخلاصة: في هذا العمل تم انجاز دراسة عملية وعددية لتحسين انتقال الحرارة باستخدام انبوب لولبي مخدد بوجود المائع النانوي. القشرة مصنوعة من الحديد المغلون ٦٥ مليمتر قطر خارجي. الانبوب مصنوع من النحاس بطول ١٠٠٠ مليمتر ،١٦ مليمتر قطر داخلي مكافئ و ١٧ مليمتر قطر خارجي تم تثبيته داخل القشرة. استخدم البخار كمصدر حراري على السطح الخارجي للانبوب حيث تم الحصول على درجة حرارة ثابتة لسطح الانبوب (١١٠˚C)، المائع النانوي من نوع اوكسيد التيتانيوم /ماء مقطر بتراكيز حجمية مختلفة (٠,٠٨، ٠,١، ٠,٢، ٠,٣)% و يمر داخل الانبوب عند عدد رينولدز يتراوح بين (٧٠٠٠-١٥٠٠٠). تم عزل القشرة من الخارج بعازل حراري لتقليل الحرارة المفقودة.تمت دراسة اداء المبادل الحراري ذو الانبوب اللولبي المخدد بدون ومع المائع النانوي. بينت النتائج العملية زيادة في معامل انتقال الحرارة بمقدار(٢٨-٣٣)% عند استخدام الانبوب اللولبي المخدد بدون المائع النانوي مقارنه بالانبوب الاملس،تم الحصول على اقصى زيادة في معامل انتقال الحرارة عند استخدام الانبوب اللولبي المخدد بوجود المائع النانوي وبتركيز ٠,٣% بمقدار (٢٥-٢٨)%مقارنه باستخدام الماء في الانبوب اللولبي المخدد.تم ايجاد علاقات تجريبية للماء و المائع النانوي بدلالة رقم نيسلت.تم انجاز محاكاة عددية للمبادل الحراري لتحليل جريان المائع و انتقال الحرارة باستخدام البرنامج المختص ANSYS 14, FLUENT package.هناك تطابق مقبول عند المقارنة بين النتائج العملية والعددية.

*Corresponding Author ahmed.eleiwi@gmail.com

1. Introduction

Heat exchangers are popular used in industrial and engineering applications. The performance of heat exchanger can significantly increase by the heat transfer augmentation techniques that leading to the reduction of heat exchanger size as well as operating cost. Enhancement techniques can be classified either as passive or active techniques. A passive technique which does not need any external power input, and the additional power needed to enhance heat transfer is taken from the available power in the system such as extended surfaces, treated surfaces. Active techniques which require external power such as mechanical aids, and surface vibration [1].

The spiral fluted tube is one of the important enhanced tubes that used in many engineering applications for example heat exchanger. Sang Chun Lee et al. [2] introduced an experimental study to evaluate the heat transfer and the pressure drop performance for a spirally indented tube. Ethylene-glycol-water solutions and pure water has been used as working fluid at Reynolds number range from 500 to 5000. The results showed that the heat transfer coefficient for the spirally indented tube was increased to more than 8 times of those for smooth tube. Pethkool et al. [3] performed an experimental investigation of the thermal performance, heat transfer enhancement and friction factor for a helically corrugated tube. The effects of pitch to diameter ratio (P/DH = 0.18, 0.22 and 0.27) and rib-height to diameter ratio (e/DH = 0.02, 0.04 and 0.06) for these types of tubes on the properties were examined. Water was used as the test fluid with Reynolds number range from 5500 to 60,000. The experimental results show that the Nusselt number, friction factor and thermal performance factor increase with increasing the pitch ratio (P/DH) and the rib-height ratio (e/DH). The maximum thermal performance factor of 2.33 was obtained for the enhanced tube with pitch ratio of P/DH=0.27 and rib-height ratio of e/DH=0.06.S. Hossainpour and Hassanzadeh [4] introduced a three dimensional numerical investigation for the heat transfer coefficient and friction factor in helically corrugated tubes. The length of all tubes was 500 mm and the inside diameter of tubes was 24 mm with three different rib height to diameter ratio was 0.02, 0.04, 0.06 and three different rib pitch to diameter ratio was 0.6, 0.8, 1.2. Water was used as working fluid with Reynolds number range between 25000-80000. The numerical results show that both the heat transfer coefficient and friction factor increase with increasing the rib height and decrease the rib pitch.

Recently, nanofluid is used as heat transfer enhancement. Farajollahi et al. [5] studied experimentally of the heat transfer behavior of γ-Al2O3/water and TiO2/water nanofluids in a smooth tube. The nanoparticle volume concentrations of γ-Al2O3/water and TiO2/water nanofluids vary in the range of 0.3–2% and 0.15–0.75%, respectively. Based on the results, the maximum enhancement of heat transfer coefficient was about 56% with 0.5vol. % γ-Al2O3/water and 0.3 vol. % TiO2/water nanofluids higher than those of water. Rohit Khedkar et al. [6] performed an experimental investigation of water to nanofluids heat transfer in concentric tube heat exchanger. The experiments were carried out for Al_2O_3/water nanofluid with different volume concentration (2%-3%). Nanofluids with Reynolds number range from 1000 to 5000. The experimental results show that the maximum enhancement of heat transfer coefficient 16% higher than water when used 3% volume concentration of nanofluid.

Rabienataj Darzi et al. [7] introduced numerical study of the Al_2O_3/water nanofluid flow inside the helically corrugated tube. The study was carried out for different corrugating pitch (16, 16, and 25mm) and height (1, 0.67, and 1mm) at various Reynolds number range from 10,000 to 40,000. The results show that the maximum enhancement in Nusselt number was 21% and 58% for 2% and 4% by volume concentration of nanoparticles respectively.

According to the available literature, enhancement the performance of the heat exchanger by using nanofluid flowing inside the spiral fluted tube is limited. Also, there is a shortage in numerical investigation of the present heat exchanger. Therefore, present work focused on experimental and numerical study of enhancement heat transfer coefficient in spiral fluted tube heat exchanger with and without nanofluid.

2. Theoretical Analysis

In the present study, cold fluid (water or nanofluid) flowing in tube side absorbed heat from the steam in the shell side as shown in figure (1). Steady state condition, insulated outer surface of heat exchange and no phase changer have been assumed during the analysis of present heat exchanger. Under these conditions the heat transfer rate through the present heat exchanger can be estimated by [8]:

$$Q_{con.} = \dot{m} c_p (T_{out} - T_{in}) \text{ and } Q_{wall} = \bar{h} A_s (T_s - T_b) \quad (1)$$

The properties of the test fluid during this study are calculated at the mean fluid temperature. It can be calculated by using the following equation [8]:

$$T_m = \frac{T_{in} + T_{out}}{2} \quad (2)$$

The heat transfer coefficient for the fluid can calculated as follows:

$$\bar{h} = \frac{\dot{m} c_p (T_{out} - T_{in})}{A_s (T_s - T_b)} \quad (3)$$

Where

$$A_s = \pi D_i L \quad (4)$$

Due to the complex shape of the inner side fluted tube, the concept of "volume based diameters" is used rather than the conventional diameters. It is calculated as [9]:

$$D_{vi} = \sqrt{\frac{4\,Vol.}{\pi\, L}} \quad (5)$$

Then Nesselt number for inner side can be calculated as [8]:

$$N_u = \frac{h D_i}{K_f} \quad (6)$$

The friction factor can be written as [8]:

$$f = \frac{\Delta p}{(\frac{L}{D_i})(\frac{\rho v^2}{2})} \quad (7)$$

The thermal performance factor can be expressed as [8]:

$$\eta = (Nu_a/Nu)/(f_a/f)^{1/3} \quad (8)$$

2.1. Thermo Physical Properties of Nanofluid

The value of volume concentration can be calculated as follow:

$$\varphi\% = \frac{(m_p/\rho_p)}{(m_p/\rho_p + m_{bf}/\rho_{bf})} \quad (9)$$

The thermal conductivity of nanofluid can be estimated by [10]:

$$K_{nf} = (125.62\varphi^2 + 4.82\varphi + 1)k_{bf} \quad (10)$$

The density of nanofluid can be evaluated by using the general formula for the mixture [10]:

$$\rho_{nf} = (1-\varphi)\rho_{bf} + \varphi\rho_p \quad (11)$$

The specific heat of the nanofluid can be evaluated by the following mixture rule [10]:

$$cp_{nf} = (1-\varphi)cp_{bf} + \varphi cp_p \quad (12)$$

The dynamic viscosity of the nanofluid can be estimated by [10]:

$$\mu_{nf} = (199.21\varphi^2 + 4.62\varphi + 1)\mu_{bf} \quad (13)$$

3. Numerical Simulation

The numerical simulation has been performed by using ANSYS 14, FLUENT package. The solution of conservation continuity, momentum, and energy equation are used to analyze both the flow field and heat transfer in the present heat exchanger. The present heat exchanger is drawing by using software program SOLD WORK PREMUM 2012 as shown in figure (1)

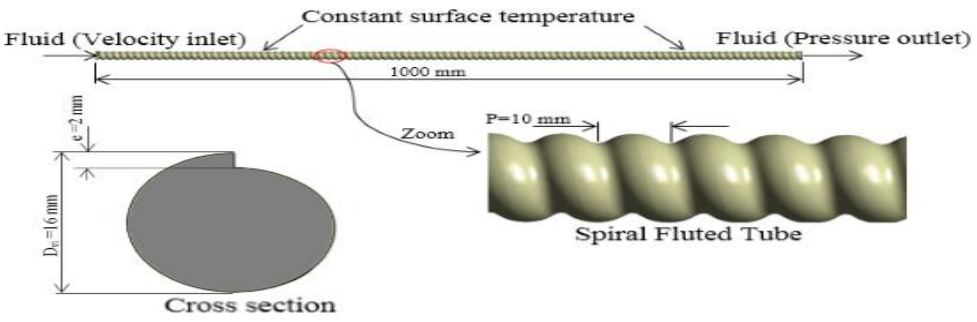

Figure (1): Spiral fluted tube heat exchanger.

3.1. Governing Equations

The flow characteristics in the present heat exchanger are assumed to be steady state, Newtonian fluid, three dimensional, and turbulent flow. The governing equation for continuity, momentum, and energy can be written as follows [11]:

Continuity equation

$$\frac{\partial u}{\partial x}+\frac{\partial v}{\partial y}+\frac{\partial w}{\partial z} = 0 \quad (14)$$

Momentum equation

$$\frac{\partial}{\partial x_j}\left(\rho u_i u_j\right) = -\frac{\partial p}{\partial x_i}+\mu\frac{\partial}{\partial x_j}\left(\frac{\partial u_i}{\partial x_j}+\frac{\partial u_j}{\partial x_i}\right)+\frac{\partial}{\partial x_j}\left(-\rho\overline{u'_i u'_j}\right) \quad (15)$$

Where:

$\left(-\rho\,\overline{u'_i u'_j}\right)$ is the Reynold's stress term which is associated with the local velocity gradients and turbulent viscosity (μ_t).

$$\left(-\rho\,\overline{u'_i u'_j}\right) = \mu_t\left[\frac{\partial u_i}{\partial x_j}+\frac{\partial u_j}{\partial x_i}\right] \quad (16)$$

Energy equation

$$\rho c_p\frac{\partial u_i T}{\partial x_i} = \frac{\partial}{\partial x_i}\left(\lambda\frac{\partial T}{\partial x_i}-\rho\,\overline{u'_i T'}\right) \quad (17)$$

3.1.1. Transports Equation for the RNG k-ε Model

$$\frac{\partial}{\partial t}(\rho k)+\frac{\partial}{\partial x_i}(\rho k u_i) = \frac{\partial}{\partial x_j}\left(\alpha_k\mu_{eff}\frac{\partial k}{\partial x_j}\right)+G_k+G_b-\rho\varepsilon \quad (18)$$

$$\frac{\partial}{\partial t}(\rho\varepsilon)+\frac{\partial}{\partial x_i}(\rho\varepsilon u_i) = \frac{\partial}{\partial x_j}\left(\alpha_\varepsilon\mu_{eff}\frac{\partial\varepsilon}{\partial x_i}\right)+C_{1\varepsilon}\frac{\varepsilon}{k}(G_K+C_{3\varepsilon}G_b)-C_{2\varepsilon}\rho\frac{\varepsilon^2}{k}-R_\varepsilon \quad (19)$$

In these equations, $\boldsymbol{\alpha_k}$ and $\boldsymbol{\alpha_\varepsilon}$ are constant and equal to 1.393.While $\boldsymbol{G_K}$ represent the generation of turbulence kinetic energy due to the mean velocity gradients and can described as:

$$G_K = \mu_t S^2 \quad (20)$$

Where:

$$S = \sqrt{\frac{1}{2}\left(\frac{\partial u_j}{\partial x_i}+\frac{\partial u_i}{\partial x_j}\right)} \quad , \quad G_b = \beta g_i\frac{u_t}{Pr_t}\frac{\partial T}{\partial x_i} \quad \text{and} \quad \mu_t = \rho C_\mu\frac{k^2}{\varepsilon} \quad (21)$$

Where: $G_b =$ is the generation of turbulence kinetic energy due to buoyancy, andμ_t the turbulent viscosity.

The additional term $R_\varepsilon$in **ε** equation is given by:

$$R_\varepsilon = \frac{C_\mu \rho \eta^3 \left(1 - \frac{\eta}{\eta_0}\right)}{1 + \beta \eta^3} \frac{\varepsilon^2}{k} \quad (22)$$

Where:

$$\eta = \frac{S}{\varepsilon} \quad (23)$$

η_0 =4.38, β=0.012 and the values of the model constants are:$C_{1\varepsilon} = 1.42$, $G_{2\varepsilon} = 1.68, C_\mu =$ 0.0845

3.2. Implementation of Boundary Conditions

Boundary conditions are specified for each zone of the computational domain as follow:

- Inlet Boundary Conditions:

The velocity inlet to the inner tube is specified during this study it is taken between (0.33 - 0.69) m/sec which is considered in experimental work. Also, the temperature inlet value to the tube is (20°C).

- Pressure Outlet Boundary Conditions:

The outlet domain is specified as pressure outlet where the pressure is assumed to be atmospheric pressure.

- Wall Boundary condition:

No slip boundary condition is specified in the wall of the inner tube. These conditions are used to bound fluid and solid region. Also, the surface temperature of the tube is (110°C).

3.3. Mesh Generation

Unstructured meshes are certainly well suited for handling arbitrary shape geometries especially for domains having high-curvature boundaries. In this study, unstructured mesh is used to discretize the computational domain by using the GAMBIT software. The most typical shape of an unstructured element is a triangle in two dimensions or a tetrahedron in three dimensions. Many other elements shapes including quadrilateral or hexahedra cells are also possible. Also, fluent can use of hybrid grids that combine different element types such as triangular and quadrilateral in two dimensions or tetrahedral, hexahedra, prisms, and pyramids in three dimensions. The choice of which mesh type to use will depend on the application. For simple geometries, quadrilateral/ hexahedral meshes can provide higher – quality solution with fewer cells than comparable triangular/ tetrahedral meshes while for complex geometries, the meshing effort by using triangular/ tetrahedral meshes **[12]**.In this study tetrahedral mesh type is used. The mesh of present model and mesh topology are shown

in figures (2) and (3) respectively .Also, during this study, many number of cells has been taken and an average of (5) million cells is found as the optimum number regarding with the best numerical prediction of present model and the maximum number of iterations done before the solver terminates. (1500) iterations are needed in this study, as shown in figure (4).

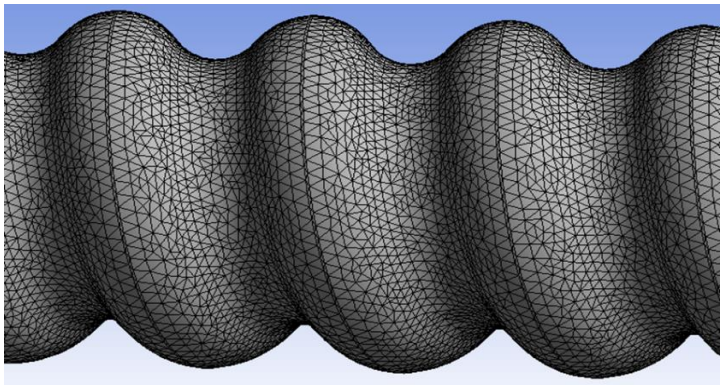

Figure (2): Mesh of present model.

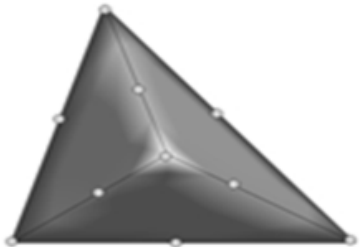

Figure (3): Mesh topology.

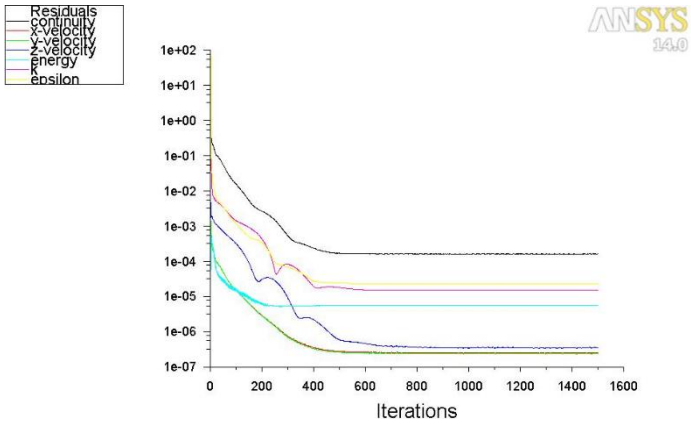

Figure (4): Residual for numerical simulation of present study.

4. Experimental setup

Figures (5) and (6) show the photograph of test rig and schematic diagram of test section. It consist test section, water supply system, steam supply system and measuring devices such as temperature recorder, water flow meter, thermocouples and manometer. The test section contains two parts, the first consists insulated shell has been manufactured from galvanized material (65 mm) outer diameter and (1000 mm) length. It is insulated from outside by fiber glass to reduce the heat losses to the surrounding. The second part is included two geometrical shapes of tubes (smooth and spiral fluted tube) are made from copper with (1 mm) wall thickness, (19 mm) outer diameter, and (1000 mm) length are used as a test tube in the present study. The spiral fluted tube has an internal envelope diameter of (16 mm), rib-height (e) of 2 mm (rib-height to diameter ratio (e/D_{vi} =0.125), and helical-rib pitch (p) of 10 mm (helical-rib pitch to diameter ratio (p/D_{vi}=0.625). The nanofluid (TiO_2/water) has been prepared by using Ultrasonic Cleaner Device. The ultrasonic cleaner device and the flask that containing nanofluid as shown in figure (7). Table (1) shown the properties of nanoparticles.

1	Tank No.1	6	Temperature Recorder	11	Test Section
2	Water Pump	7	Stand	12	Pressure Gauge
3	By-pass Valve	8	Digital Manometer	13	Tank No.2
4	Main Pumping Valve	9	Drain Valve	14	Line from the Boiler
5	Flow meter	10	Thermocouple	15	Insulation (Fiber Glass)

Figure (5): Experimental test rig.

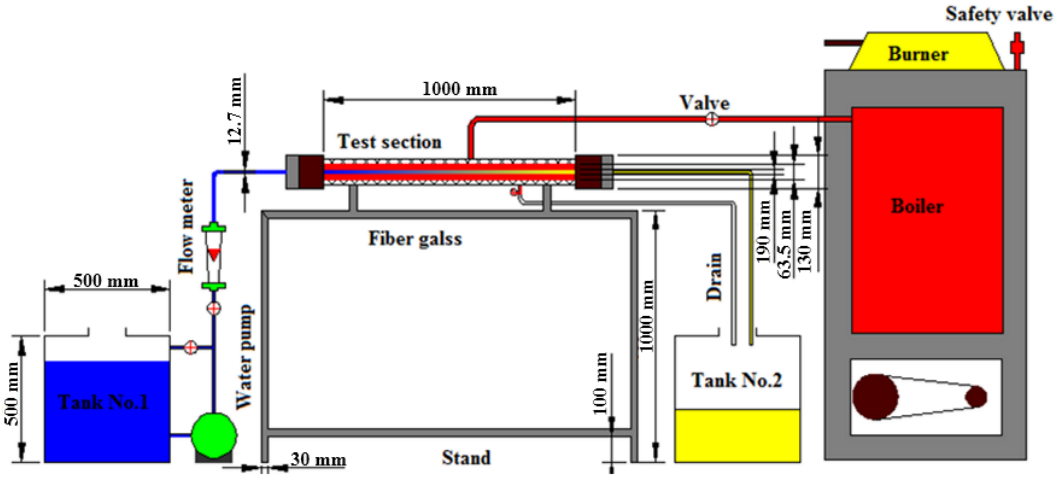

Figure (6): Schematic diagram of experimental test rig.

Figure(7):Ultrasonic with beaker

Table (1): The properties of nanoparticle.

Type	Cp(J/kg.°C)	ρ(kg/m^3)	K(W/m.°C)	Diameter(nm)
TiO_2	686.2	4230	8.9	<50

5. Results and Discussions

The performance of the present heat exchanger has been discussed through the following paragraphs.

Figures (8) and (9) show the validation of the test facility and experimental data, this obtained for smooth tube case with the previous correlations **"Dittus-Boelter** and **Petukhov"** for Nusselt number and friction factor respectively. The results show that the agreement with the above correlations, where the maximum percentage privation of 12 % and 7 % for Nusselt number and friction factor respectively.

Figures (10) explain the variation Nusselt number with the mass flow rate for smooth and spiral fluted tube. It can be seem from this figure Nusselt number increase with the increase of mass flow rate. At the same mass flow rate, the Nusselt number of the spiral fluted tube is about in range (18-24) % higher than that in the smooth tube. The spiral fluted tube provide higher turbulence intensity near the wall by recirculation flow, that lead to good mixing between all parts of the water and reduce the thermal boundary layer thickness, hence the heat transfer is increasing .

Figures (11) presented the variation of friction factor with the mass flow rate for smooth and spiral fluted tube .Obviously, for the same mass flow rate. The friction factor in the spiral fluted tube is higher than that of the smooth tube. This is a consequence of the helical rib that caused the re-circulating and turbulence flows near the tube wall which leads to difference in the viscosity effect of the fluid. The mean increase in friction factor of using spiral fluted tube is about in range (55-59) % times that of the smooth tube.

Figure (12) depicted the variation of the Nusselt number of nanofluid (TiO_2)/ water with different Reynold number and volume concentration (0.08 %, 0.1 %, 0.2%, and 0.3%) volume fractions of nanoparticles for spiral fluted tube. From this figure, it can be seen that the heat Nusselt number increases with raising both Reynolds number of nanofluid and volume concentration of nanoparticles. It can be attributed to the increase in nanoparticles concentration lead to the following results: enhancement of the thermal conductivity .Also, it causes increase the collision among nanoparticles itself and between it and tube wall that leading to rising in heat transfer rate. Generally, the maximum enhancement of Nusselt number occurs at 0.3% volume fraction of nanofluid is (30.5) % that compared with pure water. This enhancement for 0.08 %, 0.1 %, 0.2%, and 0.3% volume friction are about (6-12) %, (9 -15) %, (20-25) %, and (27-31) %, respectively.

Figure (13) demonstrated the relationship between the friction factors with Reynolds number of nanofluid for spiral fluted tube. It can be seen from the friction factor increase with rising Reynolds number. At the same Reynolds number, the friction factor decrease with increasing the volume concentration of nanoparticles, due to the increase viscosity of the working fluid that lead to increase of shear force on the tube wall. The nanofluid with the present range of volume concentration (0.08%, 0.1%, 0.2%, and 0.3%) provide frictions factors higher than the base fluid are about (24-33) %,(37-41) %, (44-47) %,(50-53) % respectively.

The Nusselt number ratio(Nu_a/Nu), defined as the ratio of the heat transfer improvement for the spiral fluted tube by using nanofluid at different volume concentrations to the Nusselt number of the spiral fluted tube for pure water versus Reynolds number, is depicted in figure

(14). It can be seen from this figure that the Nusselt number ratio decreases with Reynolds number increasing.

Figure (15) demonstrated the relationship between the friction factor ratios (f_a/f) for the spiral fluted tube versus Reynolds number of nanofluid at different volume concentrations. The result shows that the friction factor ratio decrease with the rising of Reynolds number.

Figure (16) shows the variation of the thermal performance factor (η) for spiral fluted tube versus Reynolds number of nanofluid at different volume concentrations. It can be seen from this figure the thermal performance factor decrease with Reynolds number increasing, but it increase with volume concentration of nanoparticles increasing. When the volume concentration changing lead to change in both Nusselt number and friction factor.

Figure (17) shows validation of the experimental results by numerical simulation produced by ANSYS 14, FLUENT package. The outlet temperature of inner fluid has been illustrated with Reynolds number as shown in the figure. Good agreement is observed with 12 % maximum difference between experimental and numerical results.

DGA (Dimensionless Group Analysis) program is used for development the empirical correlations to predict the Nussel number for water and nanofluid flow in spiral fluted tube respectively according to experimental data and to the algebraic expression of the form ($\boldsymbol{Y = aX_1^{N_1} X_2^{N_2} \ldots .}$)as follow:

Distilled water flow in spiral fluted tube:

$$Nu = 0.1826 Re^{0.57057} Pr^{0.476}$$

Nanofluid flow in spiral fluted tube:

$$Nu = 9.327 (Re\ \mathrm{Pr})^{0.32} (\varphi)^{0.175}$$

Above relations are valid for 9000 < Re >15000

Figures (18) and (19) show the comparison between experimental and predicted number for water and nanofluid respectively.

Figure (20) shows the temperature and velocity contours for smooth tube heat exchanger at various axial distances along the test section. From these figures can be seen that the maximum temperature appear at exist of the tube (x=100 cm). Velocity contours in this figure show that the velocity distribution at x= 0 cm is uniform. Also, fluid velocity at the center of the tube increases and then gradually decreases near the tube wall.

Figures (21) and (22) depict the temperature and velocity contours of spiral fluted tube heat exchanger with and without nanofluid respectively at various axial distances. Results showed enhancement in heat transfer over that in the smooth tube heat exchanger and the maximum temperature appear at exist of tube in the case of nanofluid. This behavior may be due to the spiral fluted tube provide better fluid mixing between the wall and the core flow region. Also, as a result of increasing the effective thermal conductivity of the nanofluid. Velocity contours in these figures reveal that the velocity distribution at x=0 cm is uniform and tend to decrease near the tube wall while it increases at the center of the tube.

Figure (23) shows the longitudinal temperature distribution contours for smooth tube, and spiral fluted tube respectively.

Figure (24) shows the velocity vector at exist of the smooth tube, spiral fluted tube heat exchanger. From this figure, it can be seen that the spiral fluted tube induced of the secondary flow and a rotational movement stronger than the smooth tube which will enhance the heat transfer rate along the tube.

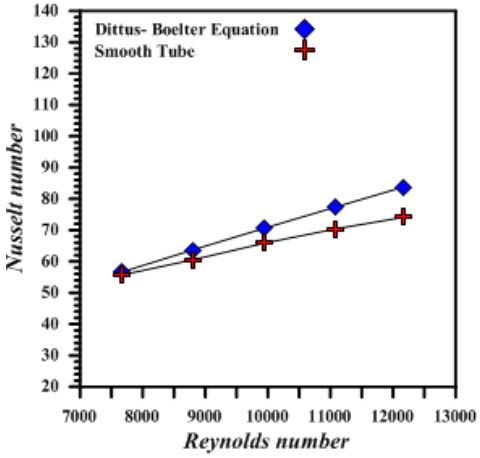

Figure (8): Comparison between experimental work and" Dittus-Boelter" equation for Nusselt number.

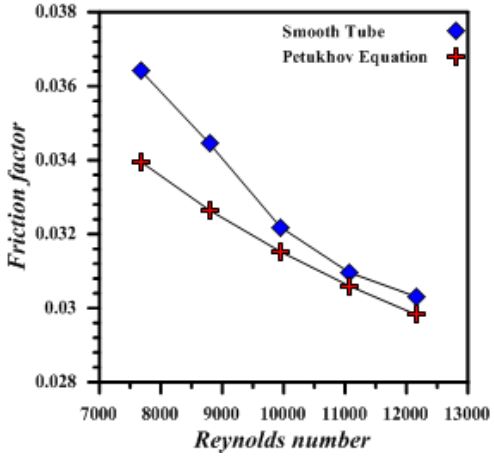

Figure (9): Comparison between experimental work and" Petukhov" equation for friction factor.

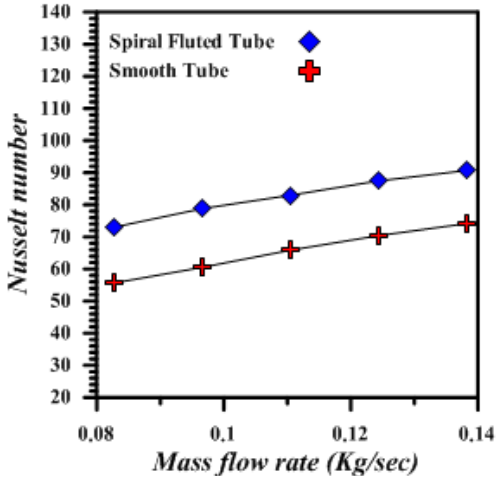

Figure (10): Effect of the geometrical shape of tube on Nusselt number.

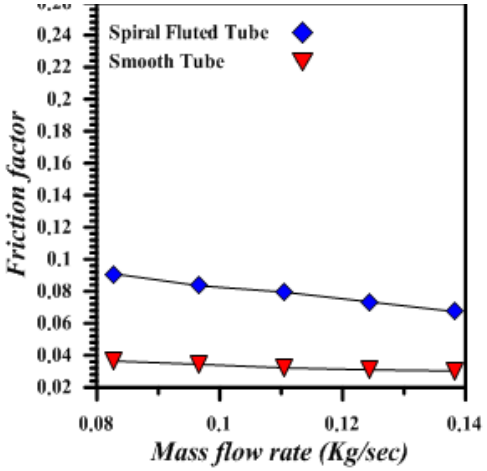

Figure (11): Variation of friction factor with different mass flow rate.

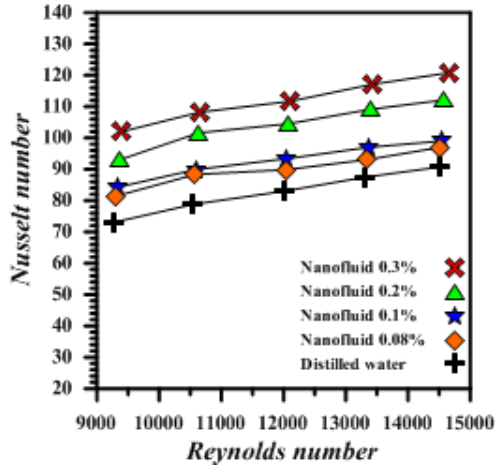

Figure (12): Variation of Nusselt number of nanofluid with Reynolds number.

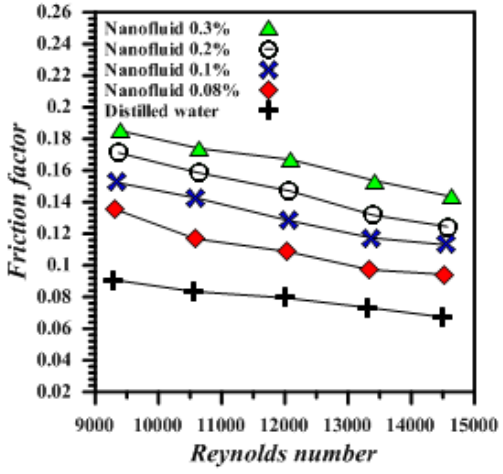

Figure (13): Variation of friction factor with Reynolds number for nanofluid.

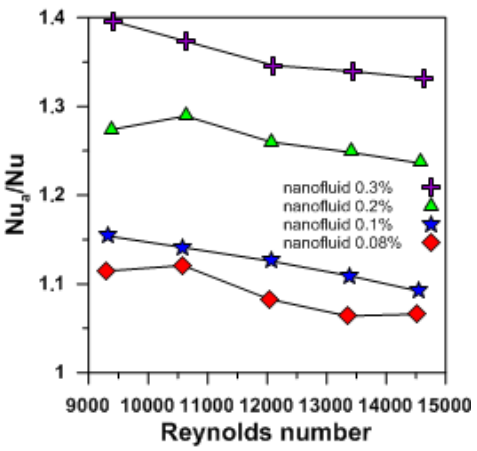

Figure (14): Variation of Nusselt number ratio with Reynolds number at various volume concentrations.

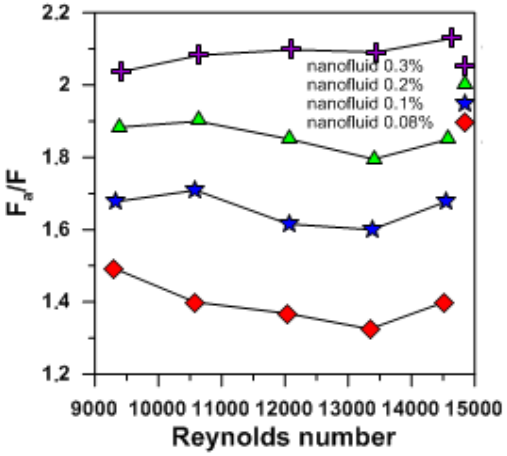

Figure (15): Variation of friction factor ratio with Reynolds number at various volume concentrations.

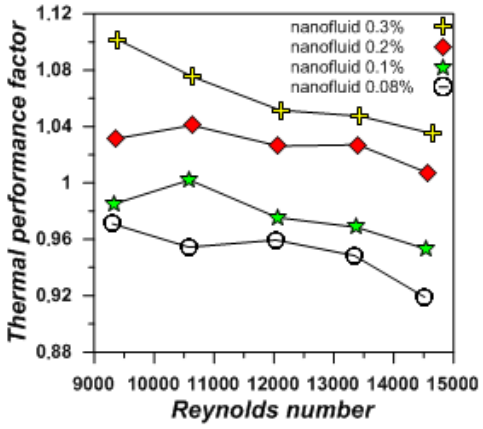

Figure (16): Variation of thermal performance with Reynolds number at various volume concentrations.

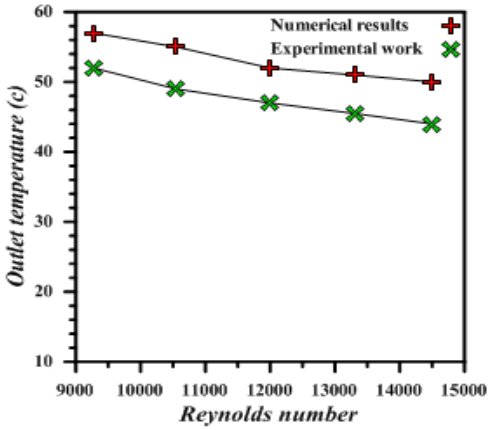

Figure(17):Comparison between experimental and simulated result.

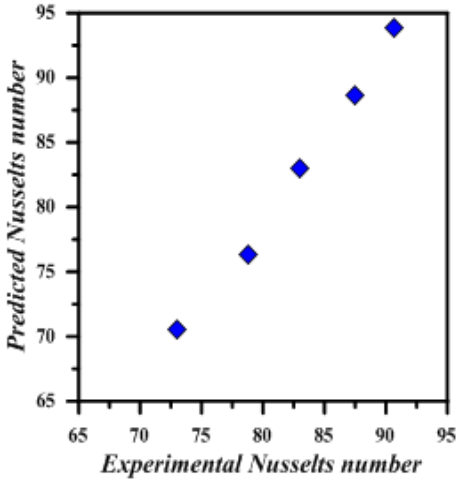

Figure (18): Comparison between predicted and experimental Nusselt number for water in spiral fluted tube.

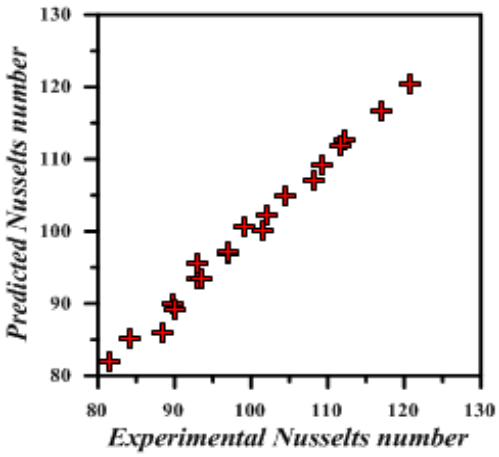

Figure (19): Comparison between predicted and experimental Nusselt number for nanofluid in spiral fluted tube.

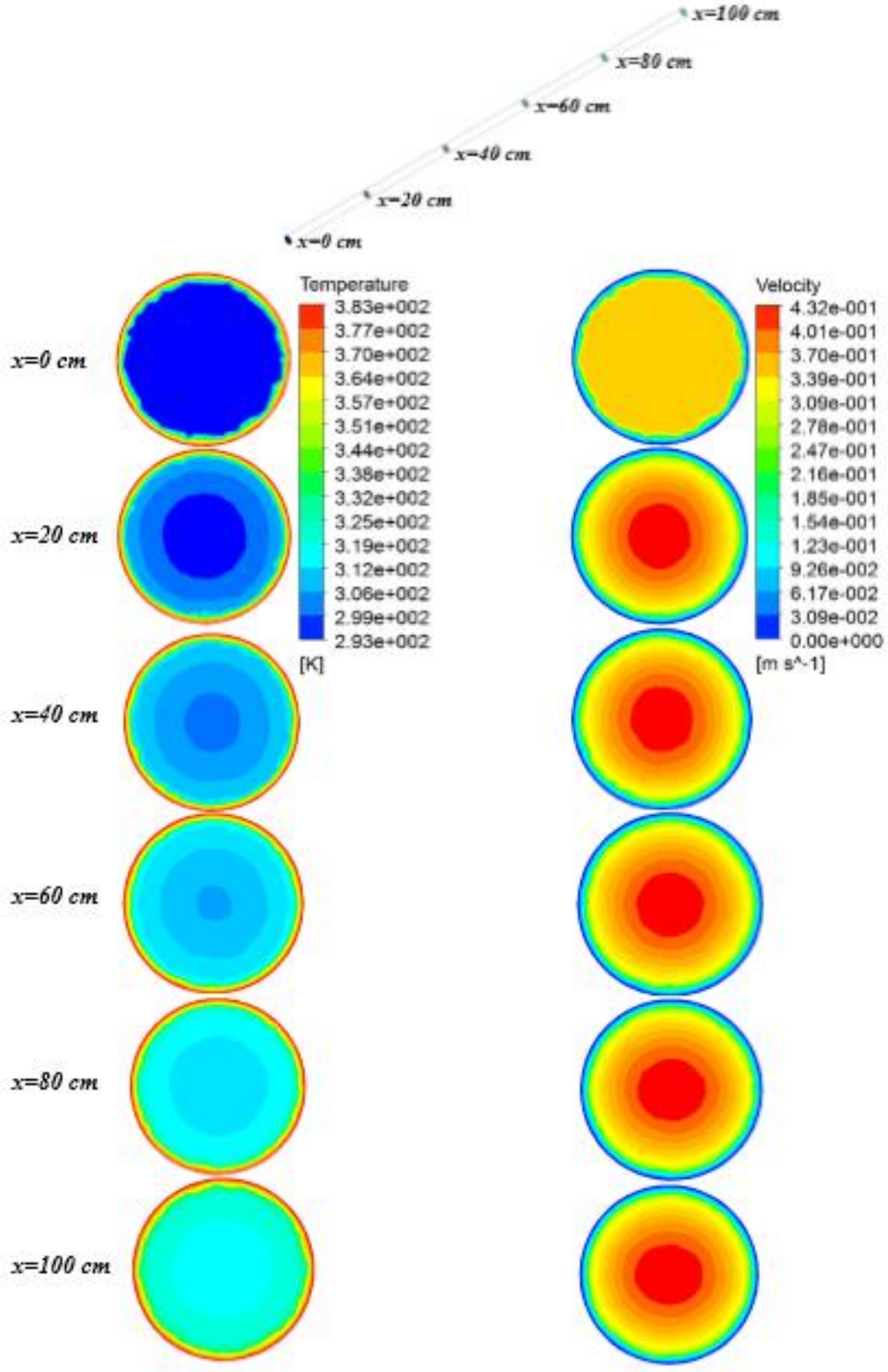

Figure (20): Temperature and velocity contours of water for smooth tube at various axial distances.

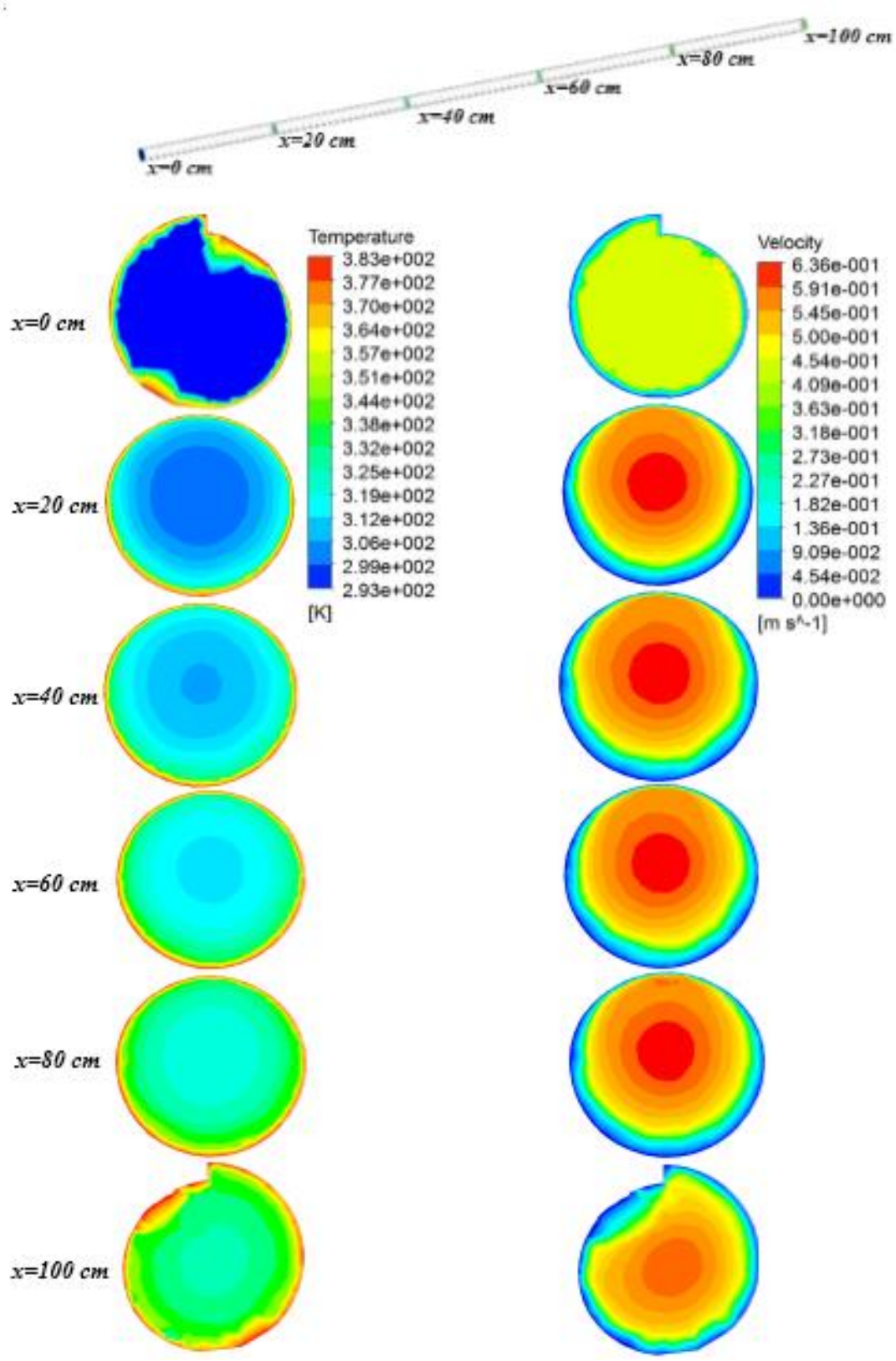

Figure (21): Temperature and velocity contours of water for spiral fluted tube at various axial distances.

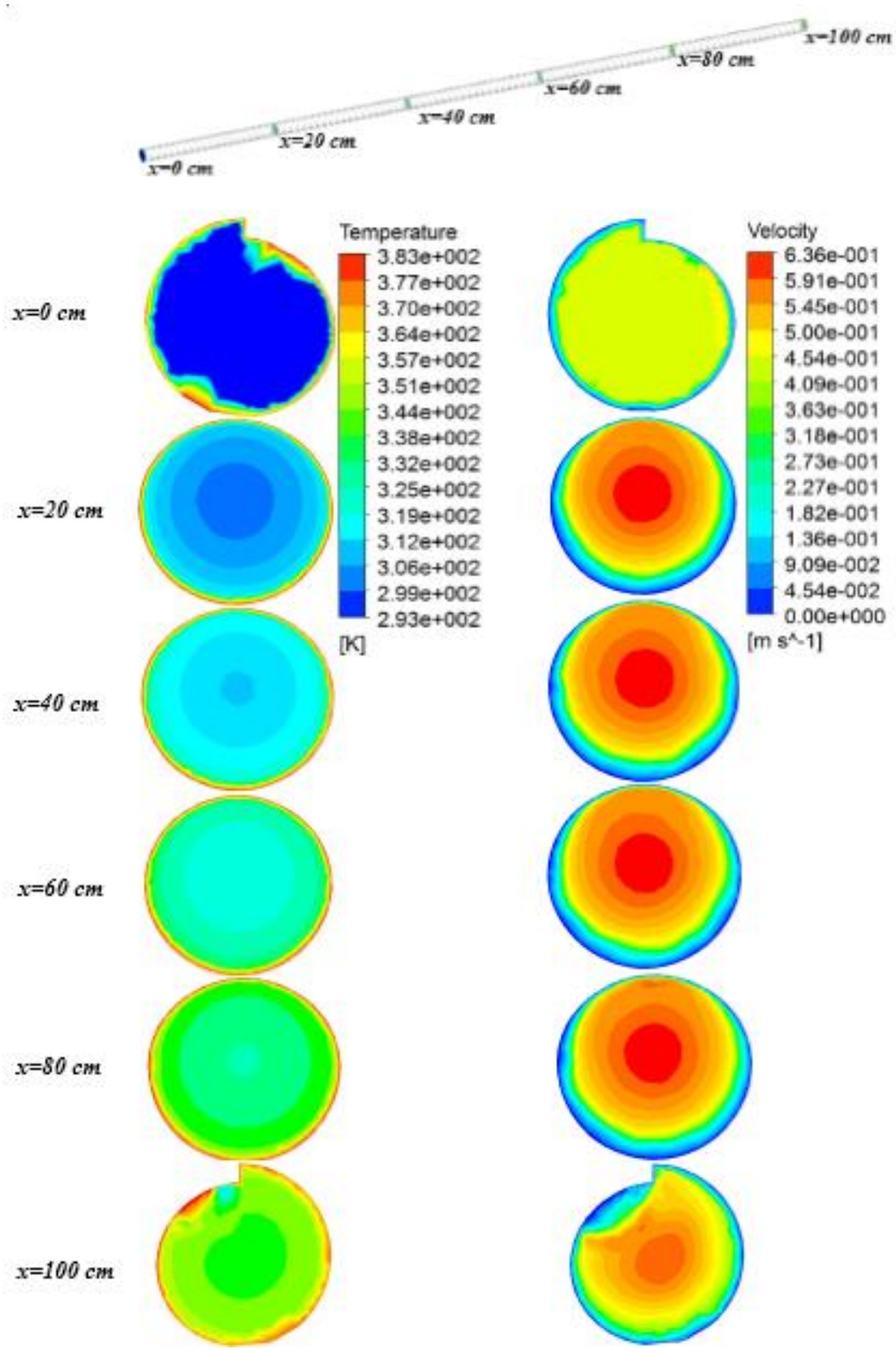

Figure (22): Temperature and velocity contours of nanofluid for spiral fluted tube at various axial distances.

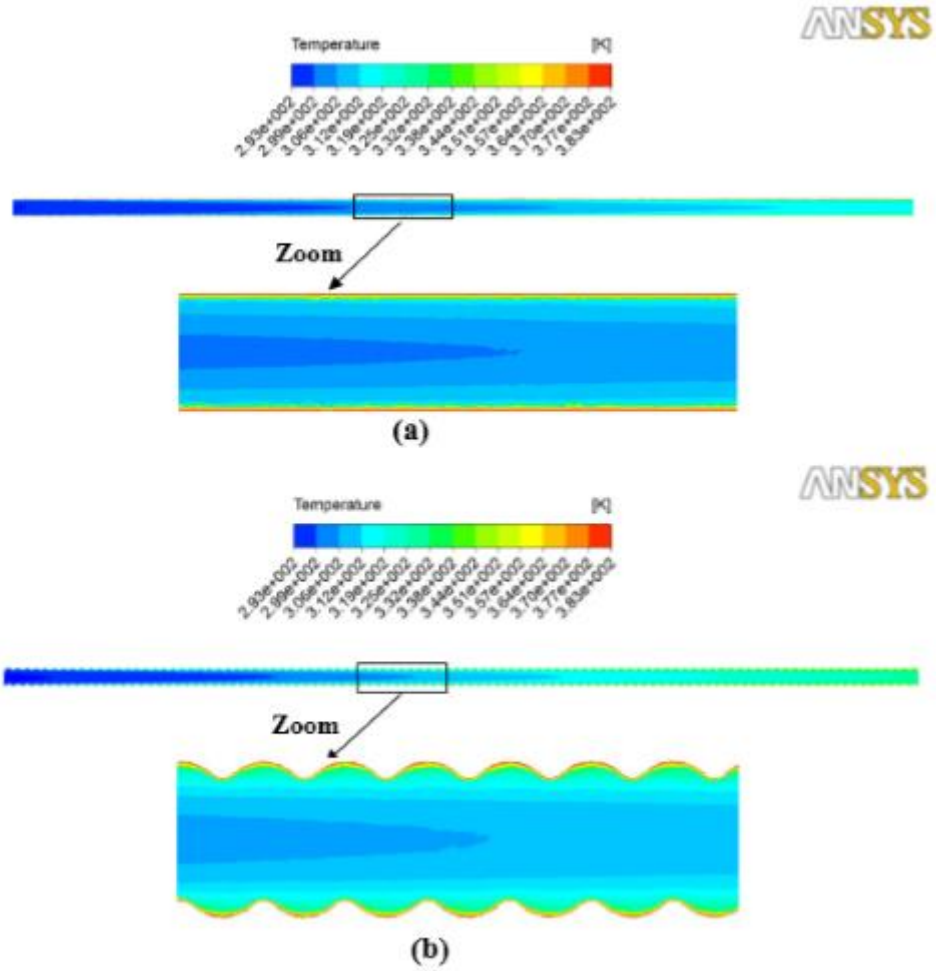

Figure (23): Temperature contours of water for (a) smooth tube and (b) spiral fluted tube.

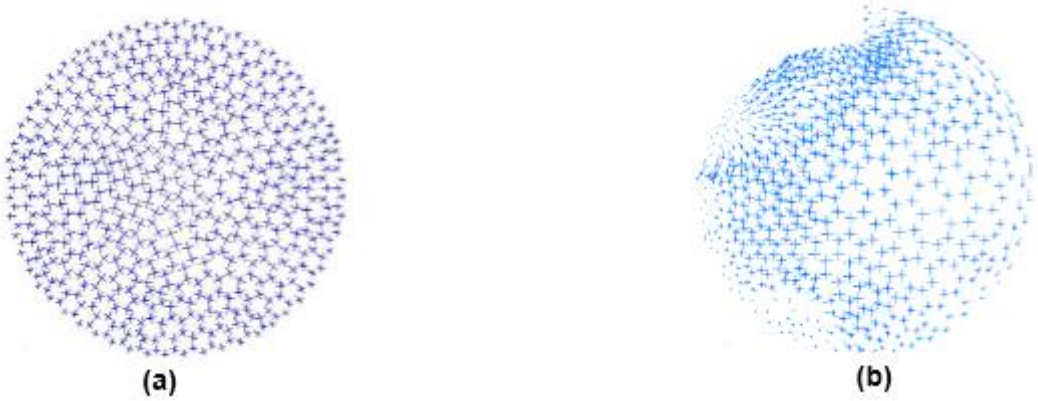

Figure (24): Velocity vectors at the exit of the test section for (a) smooth tube and (b) spiral fluted tube.

6. Conclusions

In the present work, an experimental and numerical investigation has been performed to study enhancement of heat transfer coefficient in spiral fluted tube heat exchanger with (TiO2 /water) nanofluid. The results show that the nanofluid enhances the heat transfer coefficient compared with the base fluid in general, with increase of pressure drop. The heat transfer coefficient enhanced with increasing nanoparticles concentration, and = 0.3% gives higher heat transfer enhancement among the studied concentrations. The use of the spiral fluted tube with nanofluid gives maximum thermal performance factor is around 1.1 at Reynolds number 9400 and nanoparticles concentration 0.3 %. The numerical simulation by FLUENT package generally gives numerical results in good agreement with the experimental results, and it's suitable for predicting both heat transfer and fluid flow for both nanofluid.

Abbreviations

English symbols

Symbol	Description	Units
A_s	Tube surface area	m^2
C_p	Specific heat at constant pressure	J/kg. $^{\circ}$C
$C_{1\varepsilon}$,$C_{2\varepsilon}$,C_{μ}	Turbulence constant	
D	Diameter	m
E	Rib-height	m
F	Friction factor	
$\bar{h}$	Average heat transfer coefficient	W/m^2. $^{\circ}$C
K	Thermal conductivity	W/m. $^{\circ}$C
L	Tube length	m
M	Mass	kg
$\dot{m}$	Mass flow rate	Kg/s
Nu	Nusselt number	
P	Pressure	Pa
P	Helical-rib pitch	m
Q	Heat transfer rate	W
T	Temperature	$^{\circ}$C
U	Velocity component in X direction	m/s
V	Velocity component in Y direction	m/s
W	Velocity component in Z direction	m/s

Greek Symbol

Symbol	Title	Units
ρ	Fluid Density	kg/m^3
μ	Dynamic viscosity	kg/m.s
μ_t	Turbulent viscosity	N.s/m^2
Φ	Volume concentration percentage	
Δp	Pressure difference	Pa
E	Turbulent dissipation rate	m^2/s^3
η	Thermal performance factor	

Subscripts

Symbol	Title
A	Augmentation
Bf	Base fluid
Con.	Convection
F	Fluid
I	Inner
In	Inlet
M	Mean fluid temperature
S	Surface
Nf	Nanofluid
Out	Outlet
P	Particle
v_i	The volume based inside diameter
Vol.	Volume

7. References

1. Liu, S., Sakr M. (2013). "A Comprehensive Review on Passive Heat Transfer Enhancements in Pipe Exchangers", Renewable and Sustainable Energy Reviews, Vol. 19, PP. 64-81.
2. Sang Chun Lee, Sang Chul Nam and Tae Gon Ban (1998). "Performance of Heat Transfer and Pressure Drop in a Spirally Indented Tube", KSME International Journal, Vol. 12, No. 5, pp. 917-925.
3. Pethkool, S., Eiamsa-ard, S., Kwankaomeng, S. Promvonge, P. (2011). "Turbulent Heat transfer Enhancement in a Heat Exchanger Using Helically Corrugated Tube", International Communications in Heat and Mass Transfer, Vol. 38, PP.340–347.
4. Hossainpour, S. and Hassanzadeh (2011). "Numerical Investigation of Tub Side Heat Transfer and Pressure Drop in Helically Corrugated Tubes ", International Journal of Energy and Environmental Engineering, Vol. 2, No.2, PP. 65–75.
5. Farajollahi, B., Etemad, S. Gh., Hojjat, M. (2010)." Heat Transfer of Nanofluids in a Shell and Tube Heat Exchanger ", International Journal of Heat and Mass Transfer, Vol. 53, PP.12–17.
6. Rohit, S. Khedkar, Shriram S. Sonawane, Kailas L. Wasewar (2013)." Water to Nanofluids Heat Transfer in Concentric Tube Heat Exchanger: Experimental Study", Procedia Engineering, Vol.51, PP.318-325.
7. Rabienataj Darzi, A.A., Mousa Farhadi, Kurosh Sedighi, Shahriar Aallahyari, Mojtaba Aghajani Delavar (2013)."Turbulent Heat Transfer of Al_2O_3–water Nanofluid inside Helically Corrugated Tubes: Numerical study "International Communications in Heat and Mass Transfer, Vol. 41, PP. 68–75.
8. Incropera, F. P., DeWitt, D.P., Bergman, T.L., Lavine, D.S. (2011). "Fundamentals of Heat and Mass Transfer", Seven Edition, John Wiley & Sons, New York.
9. Rousseau, P. G., Greyvenstein, G. P., Eldik, Van, M. (2000). "Detailed Simulation of Fluted Tube Water Heating Condensers", International Refrigeration and Air Conditioning Conference at Purdue University, West Lafayette, IN, USA- July 25-28.

10. Nawaf H. Saeid and Tan Heng Chia, (2011)." Investigation of Thermal Performance of Air to Water Heat Exchanger Using Nanofluids" IIUM Engineering Journal.
11. ″ANSYS FLUENT Theory Guide″ (2011). Ansys Inc., South Pointe 275 Technology Drive Canonsburg.
12. Versteeg, H. K., Malalasekera, W. (2007). "An Introduction Computational Fluid Dynamics - The Finite Volume Method", Second Edition, Prentice Hall, Pearson